Chapter 5

Further validation of the Grisham algorithm

In this chapter, three further examples, some with experimental evidence, are selected from the literature in an attempt to further validate the Grisham algorithm. The first of the three examples is taken from the NACA Technical Notes [3]; the second example is taken from a report by Tsongas and Ratay: *Investigation of diagonal tension beams with very thin stiffened webs* [13] and the last example is taken from Mason *et al.*: *The application of non-linear analysis techniques to practical structural design problems* [14].

5.1 Example 1 [3]

In this example one of the test beams used in the NACA test program is analyzed. In the NACA program, about 50 beams were tested. These can be divided into three different groups: medium sized beams which are either 635 mm (25 in) or 1016 mm (40 in) deep, small, heavily loaded beams which are 308.4 mm (12 in) deep and large beams which are 1905 mm (75 in) deep. In this example, a 1016 mm (40 in) deep beam with double uprights, designated by the NACA test program as: I-40-4Da, is evaluated. Reference [4] also contains measured stress results for the uprights and measured deflections which will be compared to the results of the Grisham algorithm.

A schematic layout of the five panel test beam is shown in Figure 5.1. The dimensions are:

1. $l = 2540$ mm (100 in)
2. $h = 1094.7$ mm (43.1 in)
3. $h_e = 1051.6$ mm (41.4 in)
4. $h_c = 942.3$ mm (37.1 in)
5. $d = 508$ mm (20 in)
6. $t = 0.99$ mm (0.039 in)

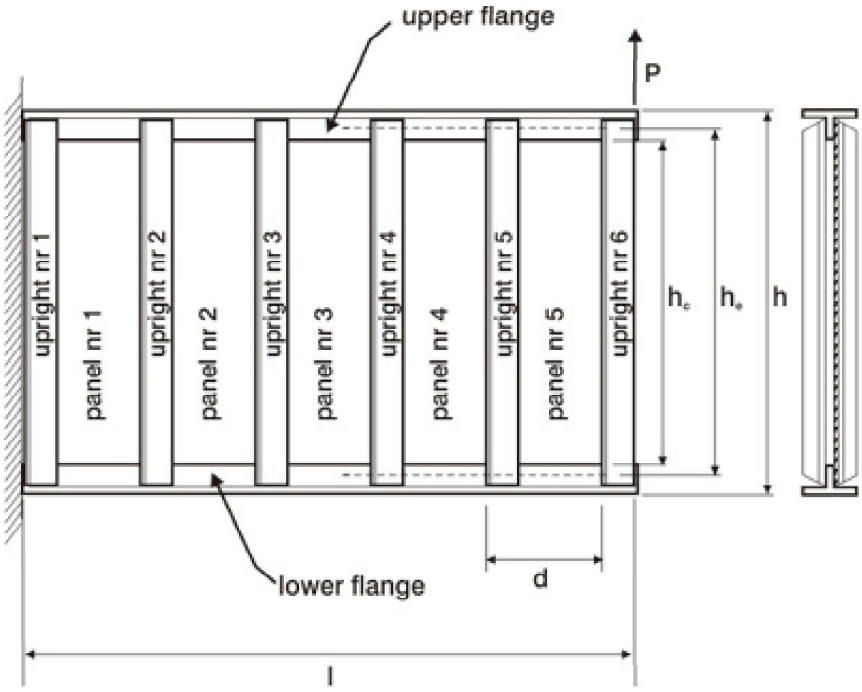

Figure 5.1: The NACA I-40-4Da test beam

7. $A_{fl} = 2293.3$ mm^2 (3.554 in^2)
8. $A_{fu} = 2293.3$ mm^2 (3.554 in^2)
9. $A_u = 227.7$ mm^2 (0.353 in^2)

The flanges are fabricated from steel while the web and uprights are fabricated from 2024-T3 alloy, with the following material properties:

1. $\sigma_{yt} = 289$ MPa (42 ksi)
2. $\sigma_{ut} = 441$ MPa (64 ksi)
3. $E_w = 72.4$ GPa (10 500 ksi)

Both flanges have a T-shaped cross-section (two angles, 76.2 mm $\times$ 76.2 mm $\times$ 7.94 mm or 3 in $\times$ 3 in $\times$ $\frac{5}{16}$ in). The uprights also have a T-shaped cross-section (two angles, 19.05 mm $\times$ 15.88 mm $\times$ 3.175 mm or $\frac{3}{4}$ in $\times$ $\frac{5}{8}$ in $\times$ $\frac{1}{8}$ in). The beam eventually failed due to column failure of the uprights at a load of 135.8 kN (30.3 kips). This load is designated the "design ultimate load" in the analysis. Two additional failure modes of the test beams are: forced crippling of the uprights and web failure.

5.1.1 The finite element model

The flanges are modelled using second order beam elements, having a T-shaped cross-section in the linear finite element analysis. The double uprights (two angles on each side of the web)

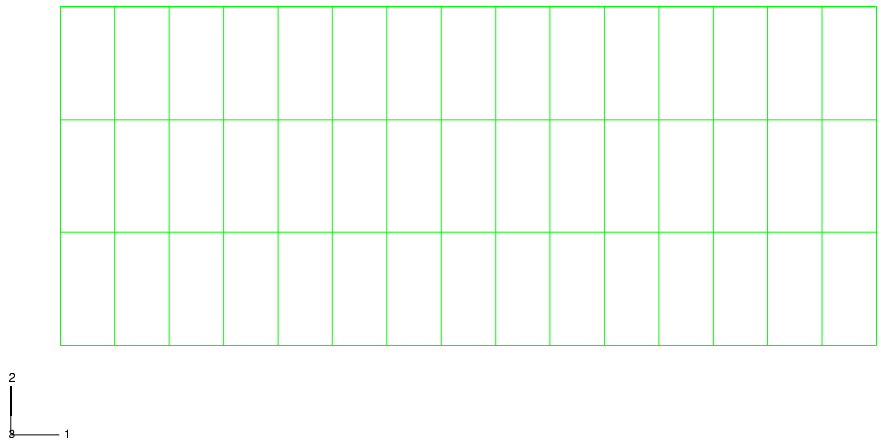

Figure 5.2: Mesh of finite element model

are also modelled with second order beam elements, having a T-shaped cross-section. The thin web is modelled with second order thin shell elements having eight nodes per element. Small displacement theory is used. The shear load is applied vertically and distributed along all the nodes at the end of the beam. Plasticity effects are not taken into account and buckling of the uprights is also not considered. NACA assumes that the web edges are clamped for calculating the critical shear and compression stress values in this example. Figure 5.2 shows the finite element mesh for the linear analysis used in the Grisham algorithm.

5.1.2 Web results

Figures 5.3 through 5.7 show the stresses in the web after completion of the analysis. Figures 5.8 and 5.9 show a vector plot of the maximum and minimum stresses in the web respectively.

In Table 5.1, the web results for the panels obtained using the iterative procedure of Grisham are compared with that of the NACA approach [3]. The correlation is good. No experimental results from the NACA tests are available for the webs. Again, the results for panels 1 and 5 are ignored since they include edge effects that are automatically included via the finite element analysis and are not accounted for in the NACA approach. The results for the three panels using Grisham's algorithm are very close to the results obtained using the NACA method.

The critical shear stress value τ_{cr} using the Grisham algorithm is $\tau_{cr} = 2.568$ MPa while the NACA procedure gives a value of $\tau_{cr} = 2.868$ MPa. The Grisham algorithm value is based on analytical relations that depend on geometry and material properties. The NACA

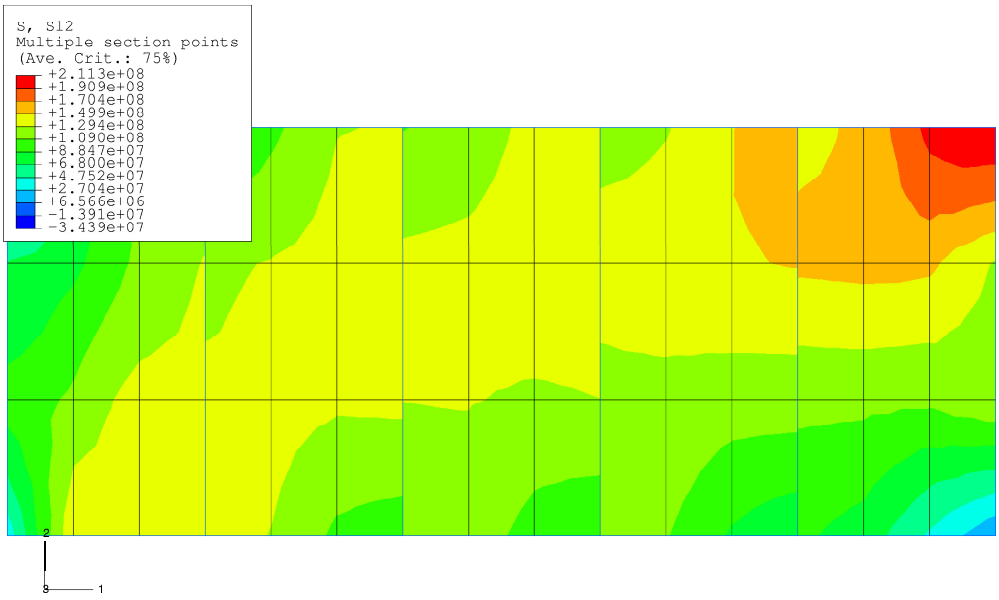

Figure 5.3: Unsmoothed shear stress distribution (τ_{xy}) in the web after the final iteration

approach uses analytical as well as empirical relations to calculate the critical shear stress. Table 5.2 shows some additional output data from the Grisham algorithm: the diagonal tension and compression-compression buckling stress values for each panel. The Modified Wagner and NACA methods do not produce values that can be compared to this data. As in the verification example, the final compressive stress values are very low. This indicates that the compressive-compressive buckling effects are insignificant in this example.

	Grisham algorithm			
	Panel 2	Panel 3	Panel 4	NACA [3]
k	0.673	0.667	0.657	0.680
α [degrees]	40.29	40.32	40.39	39.00
τ_{xy} [MPa]	127.93	128.19	128.13	129.62

Table 5.1: Web data comparison for example 1

5.1.3 Upright results

The Grisham algorithm results for the upright stresses are given in Figures 5.11 and 5.12. Again uprights number 1 and 6 are not considered because of boundary conditions. Figure 5.10 shows the position of these section points on the cross-section of the upright as well as the position of the uprights relative to the web.

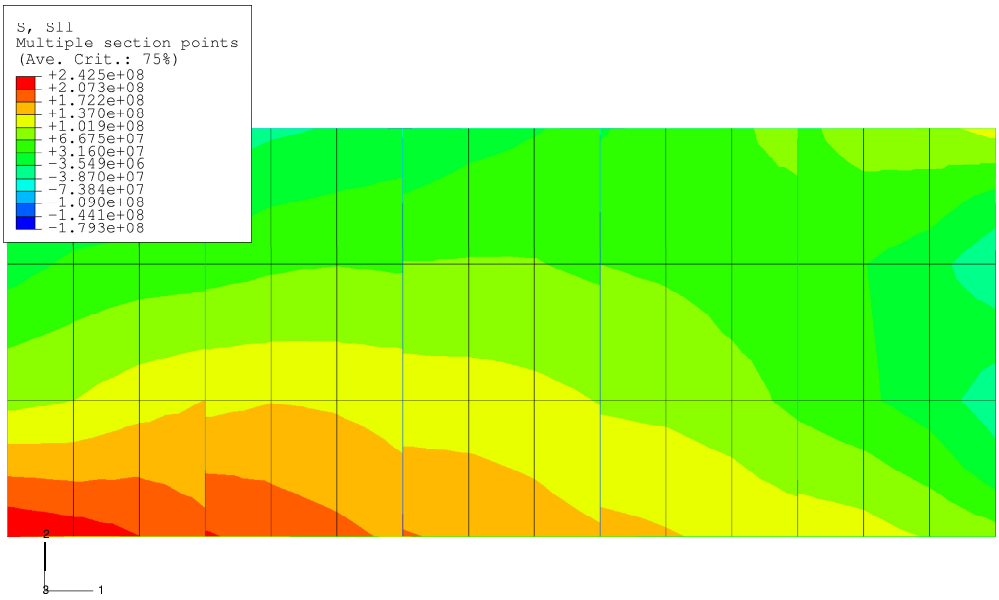

Figure 5.4: Unsmoothed normal stress (σ_x) in the web after the final iteration

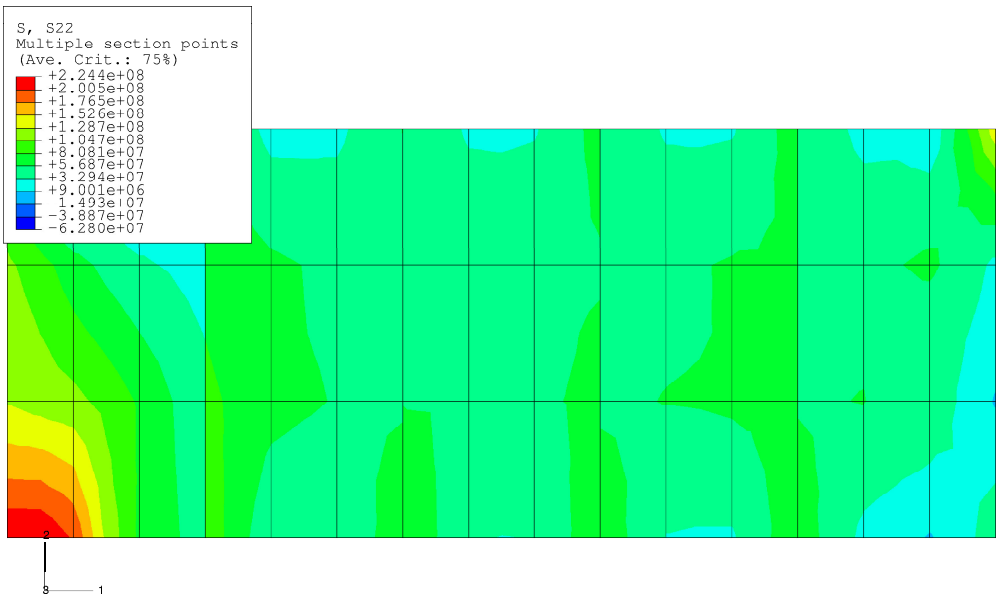

Figure 5.5: Unsmoothed normal stress (σ_y) in the web after the final iteration

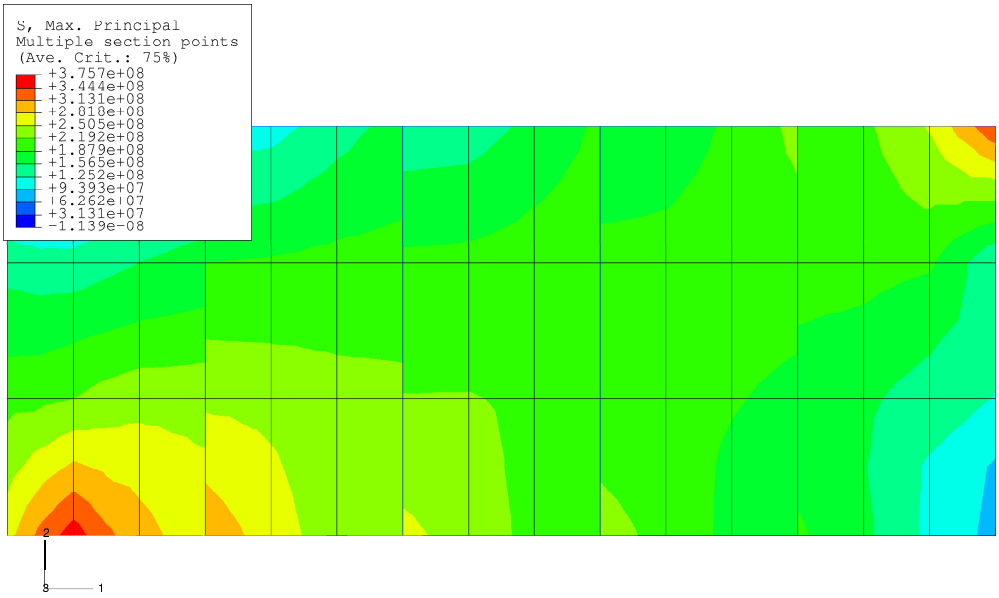

Figure 5.6: Unsmoothed maximum principal stress (σ_1) in the web after the final iteration

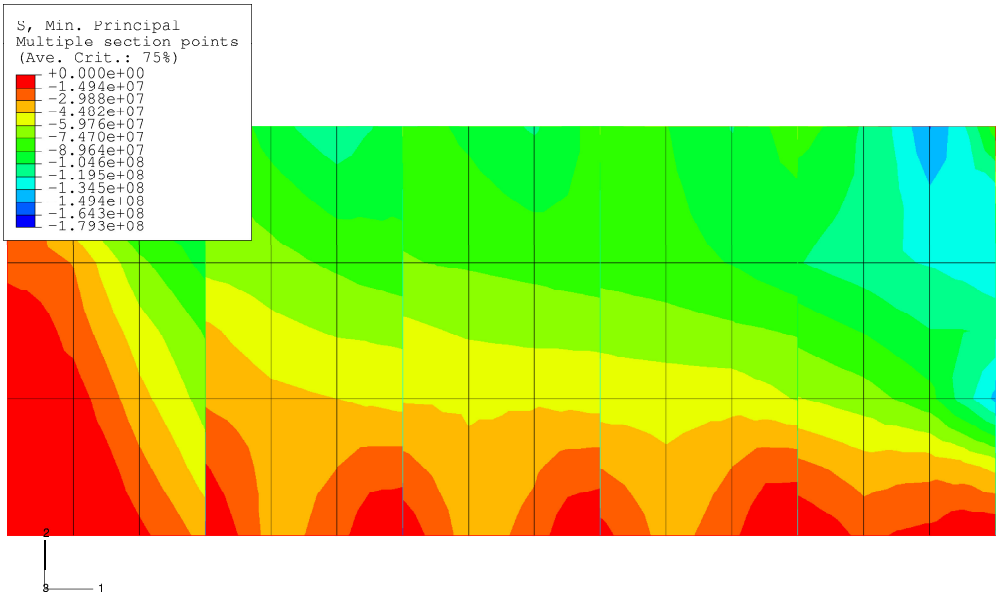

Figure 5.7: Unsmoothed minimum principal stress (σ_2) in the web after the final iteration

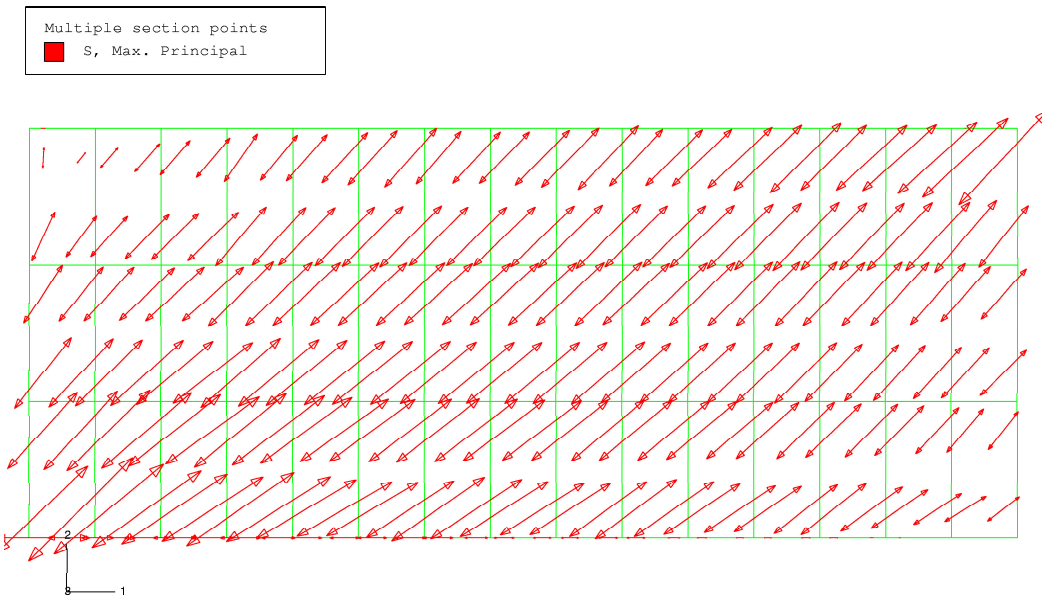

Figure 5.8: Maximum principal web stress vector plot

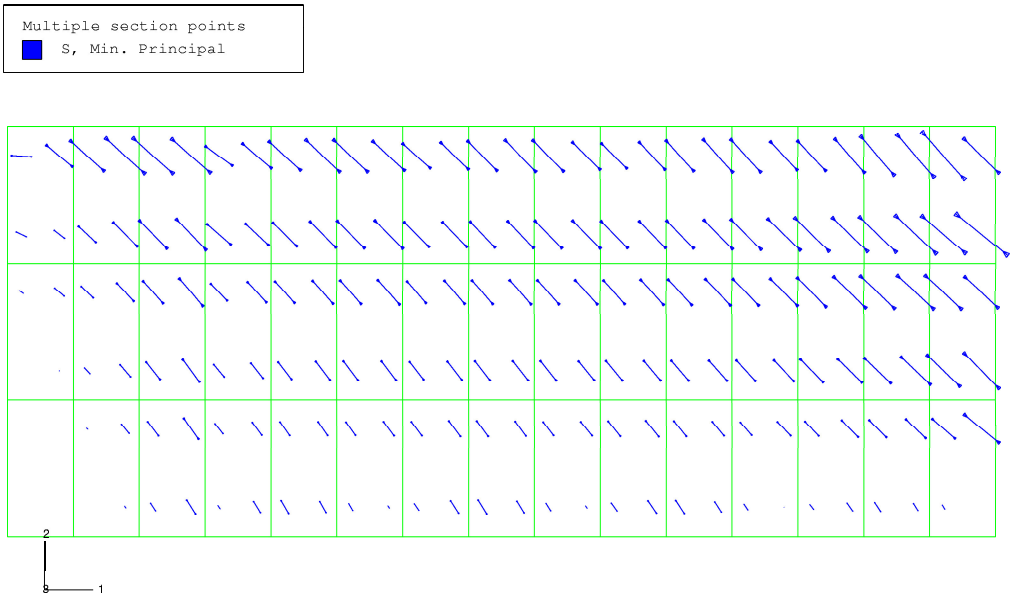

Figure 5.9: Minimum principal web stress vector plot

	Grisham algorithm		
	Panel 2	Panel 3	Panel 4
$\sigma_{x_{DT}}$ [MPa]	101.52	100.73	98.95
$\sigma_{y_{DT}}$ [MPa]	72.95	72.57	71.60
σ_{x_c} [MPa]	0.162	0.243	0.557
σ_{y_c} [MPa]	0.421	0.551	0.531

Table 5.2: Diagonal tension and compressive stress values calculated by the Grisham algorithm

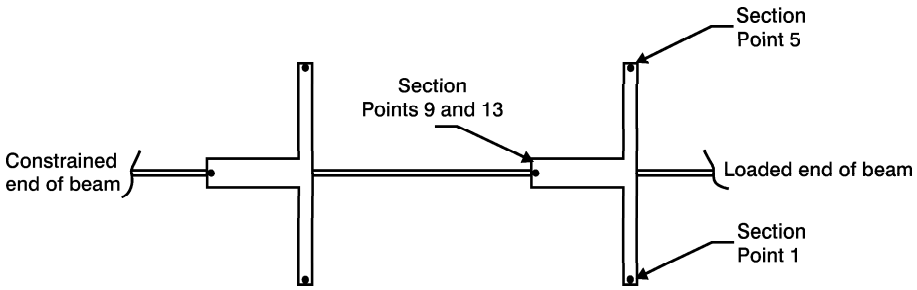

Figure 5.10: Cross-section of the upright showing the location of the section points

From the data in Figures 5.11 to 5.12 it can be seen that, for all the uprights, the values at all section points are negative and therefore in compression. The diagonal tension effects in the web tend to pull the upper and lower flanges together, loading the uprights in compression. Because there is no eccentricity here as in the verification example, and therefore no out-of-plane-bending, every point on the cross section is in compression.

The stress variation along the length of the uprights is nearly linear, increasing slightly towards the lower flange. The NACA approach, however, predicts the maximum stress value to be at a point on the neutral axis of the beam, which for this beam is half way between the two flanges.

Table 5.3 compares the results from the NACA method with the Grisham results. Measured stress values are also available from the NACA test program. The average and maximum measured upright stress as a function of load, from [4], are shown in Figure 5.13. At a load of 135.8 kN (30.3 kips) the average value is 98.6 MPa (14.3 ksi), while the maximum stress is 120.7 MPa (17.5 ksi). The average stress values for the Grisham algorithm are calculated along the length of the upright, using all the integration point values at all the section points. The measured NACA results are taken from two or three uprights in the central portion of the beam. Nine to thirteen gauge stations were used on each upright. The average measured stress in the upright is taken as the average of all the gauge readings on the beam. The Grisham algorithm results compare very well with the NACA measured results.

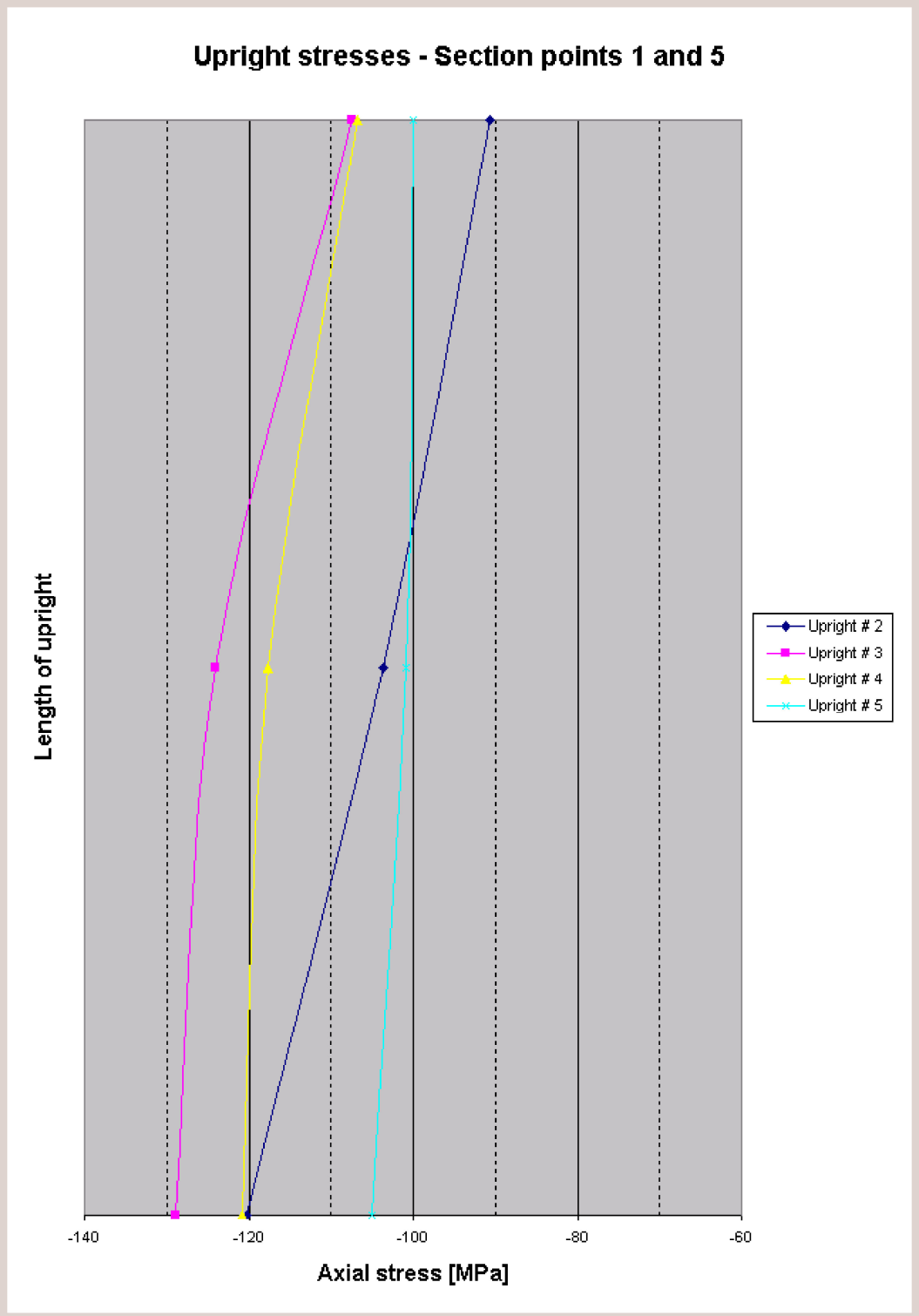

Figure 5.11: Stress along the length of the uprights at section points 1 and 5

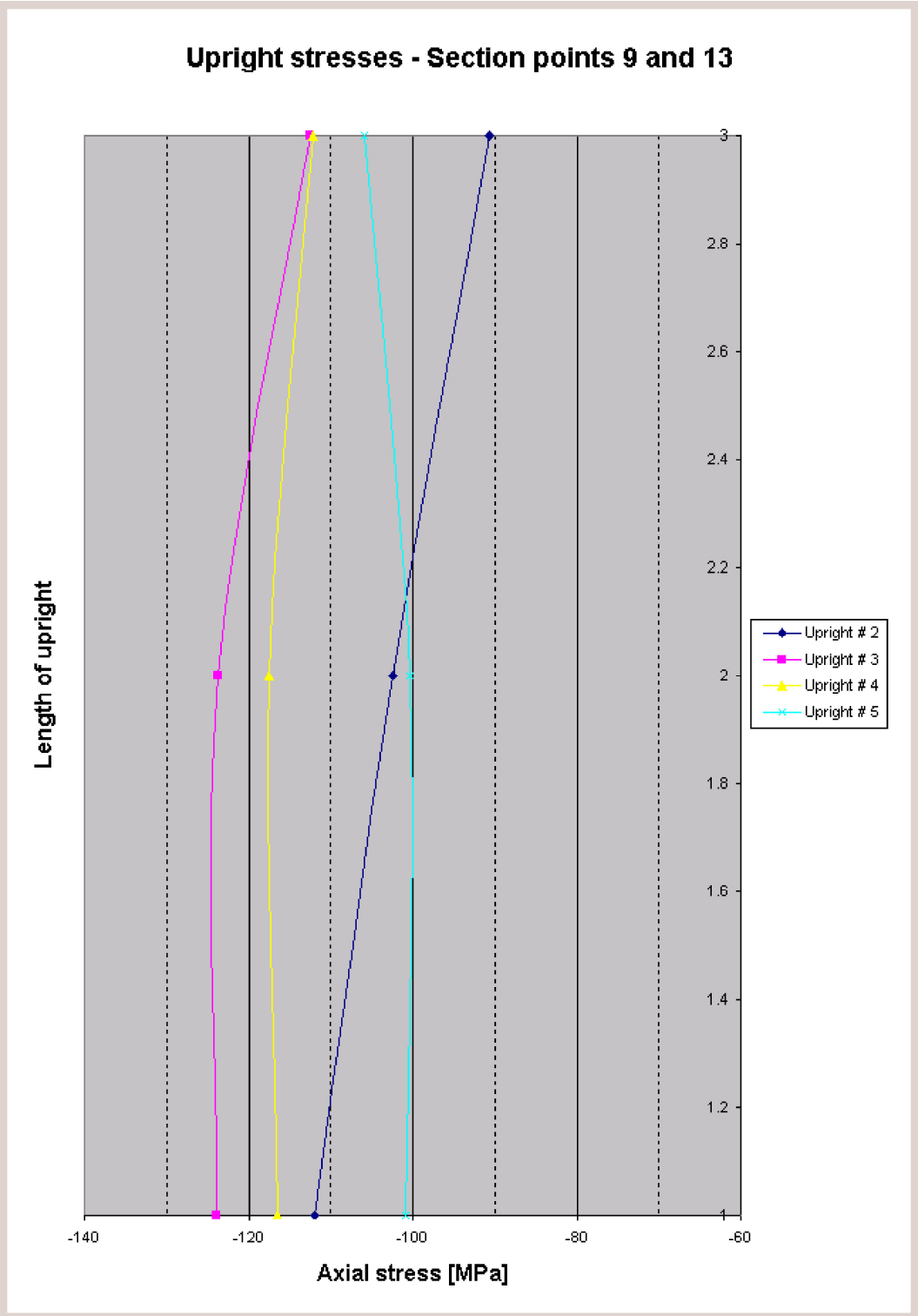

Figure 5.12: Stress along the length of the upright at section points 9 and 13

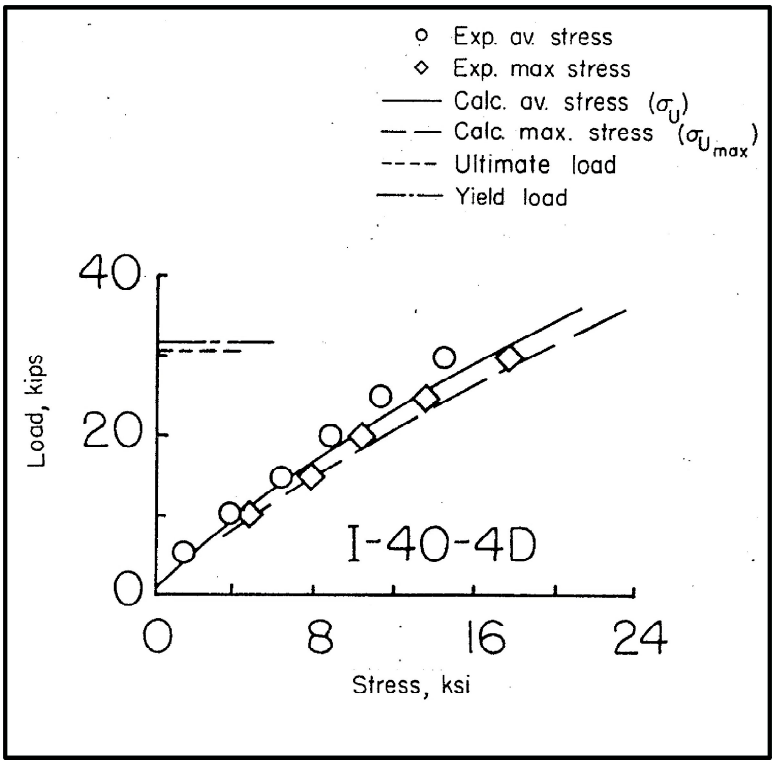

Figure 5.13: Measured upright stress data for beam I-40-4Da (Reproduced from [4])

	Grisham algorithm				NACA [3]	NACA [4]
	Upright 2	Upright 3	Upright 4	Upright 5	(theory)	(measured)
$\overline{\sigma}_u$	-94.8	-120.1	-115.2	-102.1	-116.5	-98.0
$\sigma_{u_{max}}$	-120.3	-128.9	-120.8	-105.9	-132.4	-121.0

Table 5.3: Upright stress comparison: I-40-4Da

5.1.4 Flange results

Figure 5.14 shows the bending stresses along the upper and lower flanges. The upper flange plot shows the stress in the upper fibre of the beam while the lower flange plot shows the lower fibre stress in the beam.

5.1.5 Deflection results

The experimental results for the deflection of the beam as a function of load, from Kuhn [4], are shown in Figure 5.15. From the graph the deflection at 30.3 kips is 0.85 inches which is 21.6 mm. The deflection value of the finite element analysis from the Grisham's algorithm is 28.4 mm. The displaced shape of the model at the end of the iterative analysis is shown in Figure 5.16.

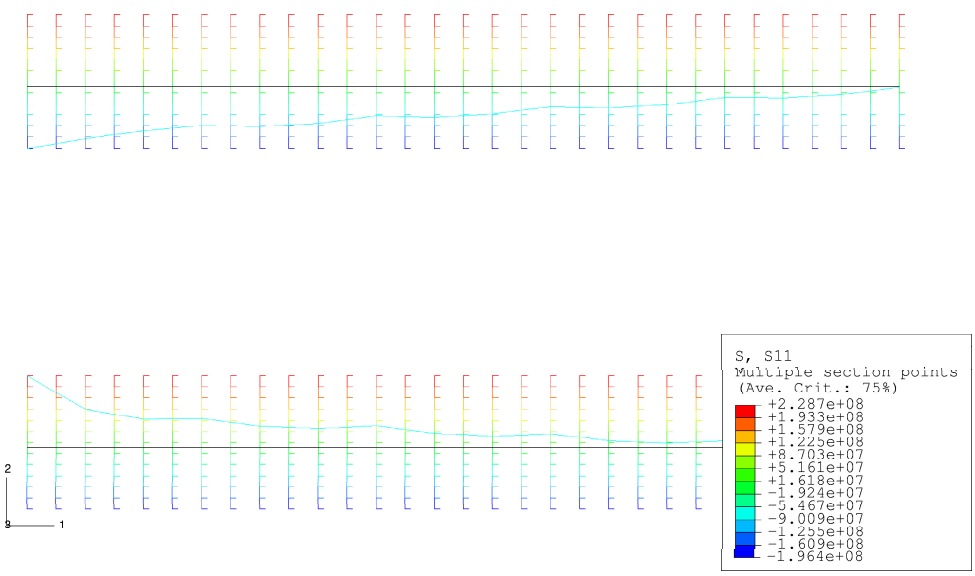

Figure 5.14: Axial stress distribution in the two flanges after the final iteration

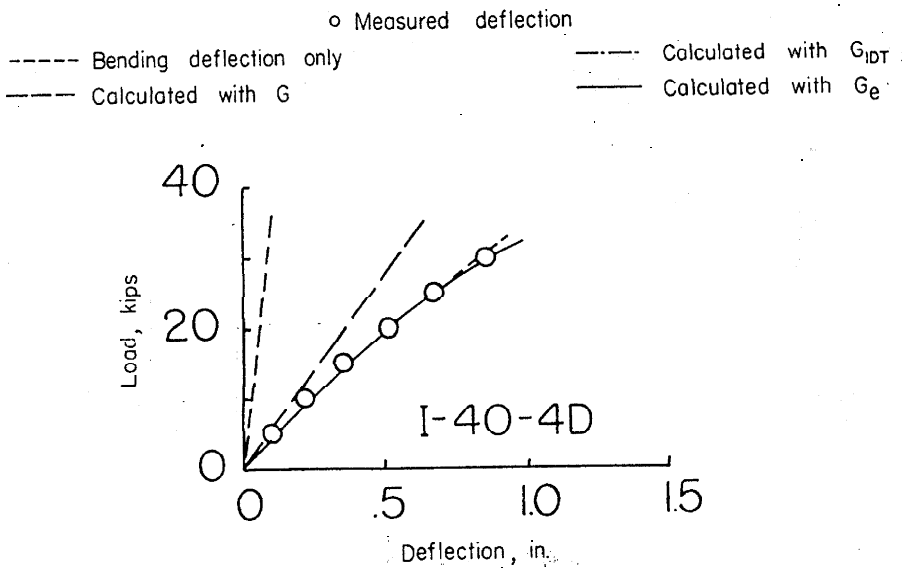

Figure 5.15: Measured deflection data for beam I-40-4Da (Reproduced from [4])

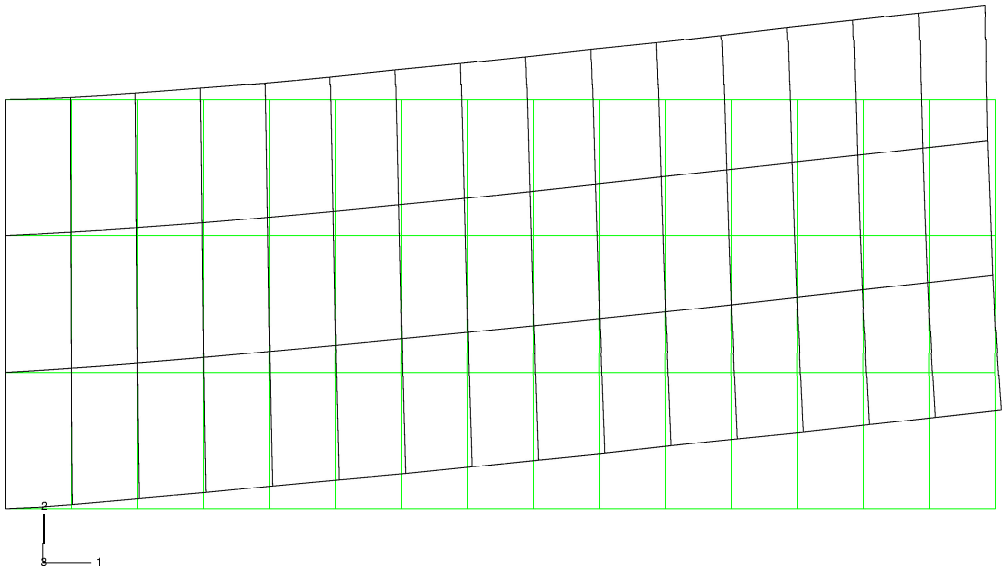

Figure 5.16: Displaced shape of the finite element model after the final iteration

5.2 Example 2 [13]

The second example, like the previous one, has experimental data that can be compared with the Grisham algorithm results (web stresses; upright stresses and shear deformation). This three panel structure, shown in Figure 5.17, has a very thin web (0.129 mm) as well as a very high aspect ratio ($\frac{L_y}{L_x}$) of 6.12, placing it outside the scope of the accepted NACA design criteria [3]. An extensive testing program (both static and fatigue) was carried out on various geometric configurations (test specimens A to M) of this structure to obtain empirical data to validate the use of the NACA design criteria for similar structures. Figure 5.18 shows a schematic layout of the test setup. Details regarding the tests can be found in [13]. This kind of deep beam structure is used in spacecraft design to ensure minimum weight. The test panels were chemically milled from 7075-T6 aluminium alloy web sheets. This allowed for very thin webs to be manufactured. The web thickness was measured, after manufacture, at various locations on the sheet and an average calculated. For test specimen C this real thickness was found to be 0.117 mm.

Test specimen C, being one of three balanced designs, having very small margins of safety for all principal modes of failure, and the one with the thinnest web, was selected for the comparative study. The specimen eventually failed in the web at a load of 44 320 N (9.96 kips). Since data at the failure load is not accurate, a load value of half the failure load was selected for the analysis.

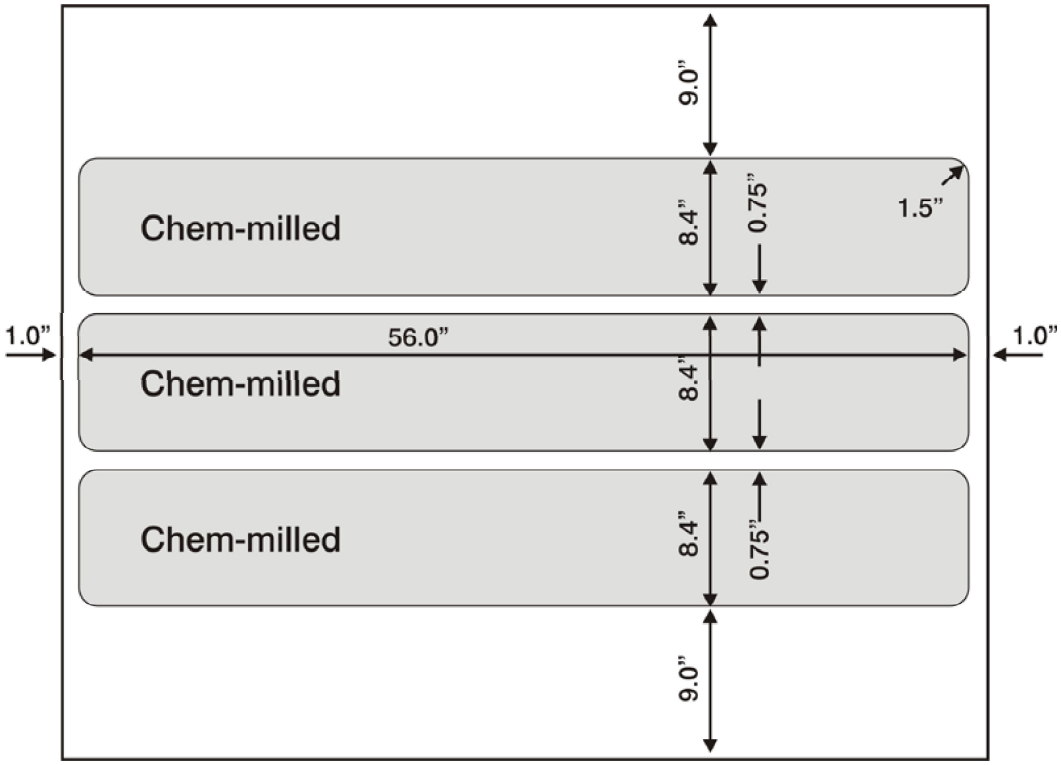

Figure 5.17: Chemically milled web sheet - test specimen C (Reproduced from [13])

5.2.1 The finite element model

The upright in this structure consists of a 'land' section that is an integral part of the web as well as a Z-shaped extruded section that is attached to the back of the 'land', resulting in an eccentric support system. The eccentricity was taken into account in the finite element model.

The measured upright stresses showed very little evidence of bending even though eccentricity is present in the structure. For this reason, second order beam elements of circular cross-section are used for the uprights in the finite element model. For simplicity, because flange stresses were not measured, the flanges are also modelled using second order beam elements of circular cross-section. Second order, thin shell elements are used for the webs. Each panel has a 3×9 web mesh density.

Figure 5.19 shows the finite element mesh for the linear model used in the Grisham algorithm. The structure is built in at the one end. At the other end, to simulate the actual testing conditions accurately, only the second degree of freedom, in which the applied load acts, is free. The applied load is evenly distributed along all the nodes.

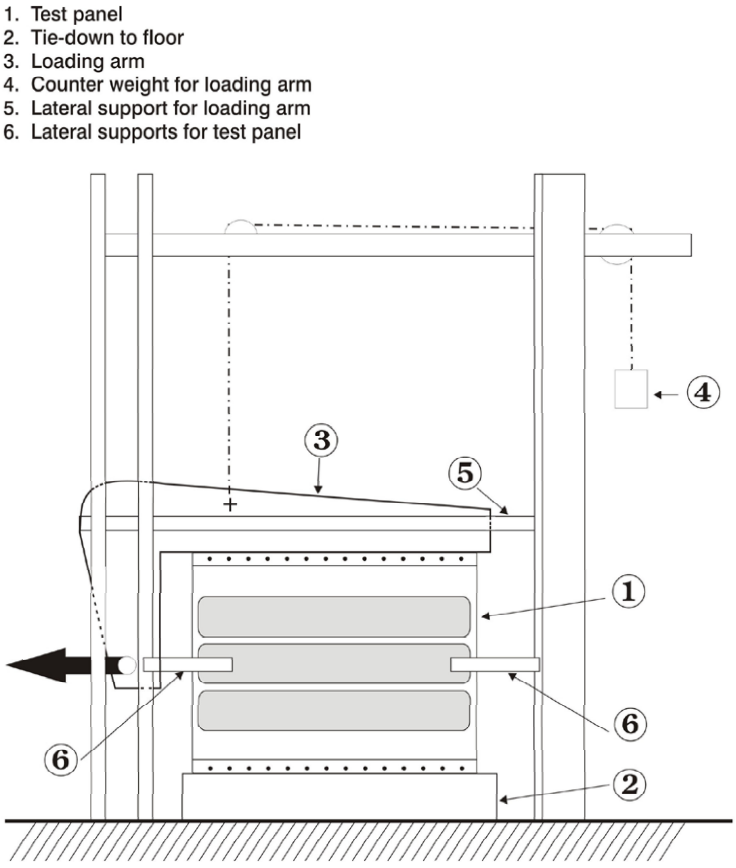

Figure 5.18: Schematic drawing of the test setup (Reproduced from [13])

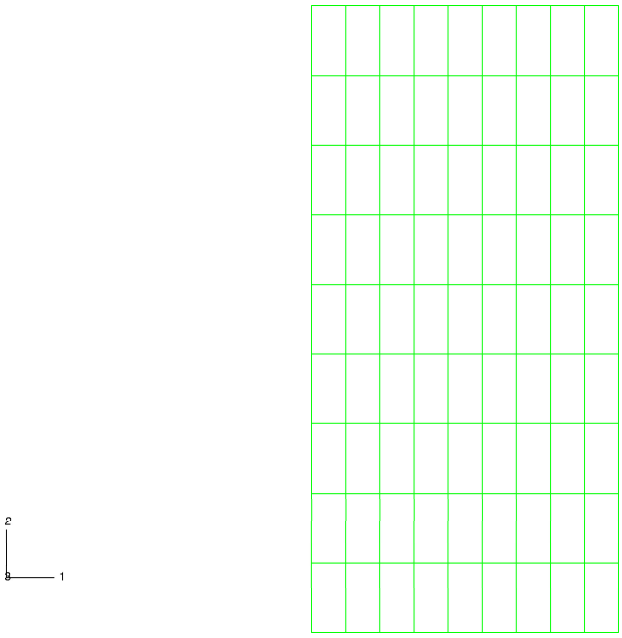

Figure 5.19: Mesh of finite element model

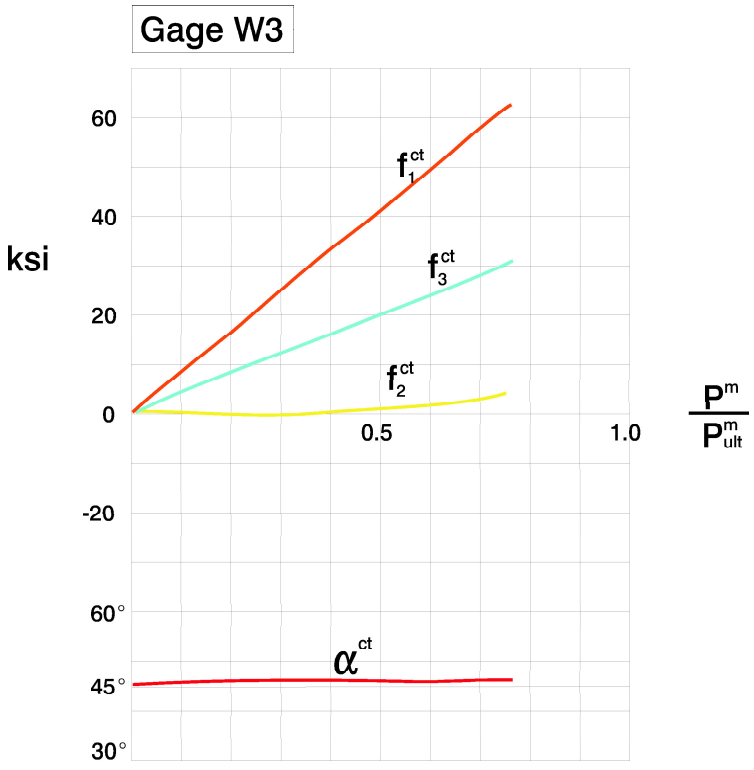

Figure 5.20: Magnitude and direction of the principal stresses in the web (Reproduced from [13])

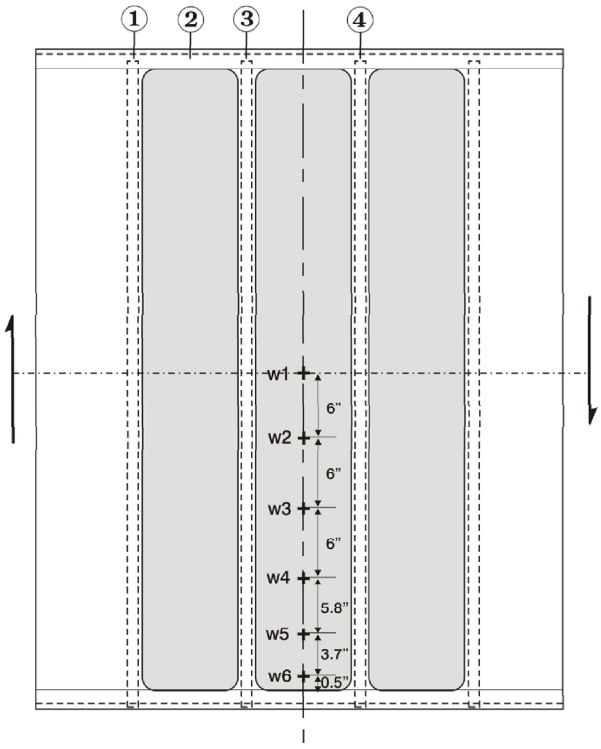

Figure 5.21: Strain and dial gauge locations on the test specimen (Reproduced from [13])

5.2.2 Web results

We now consider experimental data. Figure 5.20 shows the measured web results of the chemically milled sheet from strain gauge station 'W3'. Figure 5.21 shows the locations of the various strain gauge stations on the chemically milled web test piece. Stations 'W1' to 'W6' all had very similar results. According to Figure 5.20 the minimum principal stress (f_2^{ct} in the figure) remains close to zero for the duration of the test, while the maximum principal stress (f_1^{ct} in the figure) increases almost linearly. At half the failure load, 4.98 kips (22 160 N), which is also the load used in the finite element analysis, the maximum principal stress has a value of $\sigma_1 = 40$ ksi (275.8 MPa). The angle of major principal stress α^{ct}, as measured from the flange line and computed from gauge readings, remains just above 45 degrees for the duration of the test.

Figures 5.22 to 5.28 show the Grisham algorithm stress results in the web after the final iteration. Figure 5.25 gives a contour plot of the maximum principal stress in the web and shows this stress value in the middle bay to be in the range of $\sigma_1 = 279.0$ MPa to $\sigma_1 = 325.5$ MPa. The measured value is $\sigma_1 = 275.8$ MPa. Figure 5.26 gives a contour plot of the minimum principal stress in the web. Like the measured value this stress is compressive and only slightly less than zero in the middle bay. Figures 5.27 and 5.28 show the vector plots of the principal stresses in the web and clearly show the large difference in magnitude.

The angle of major principal stress calculated from the web results of the Grisham approach

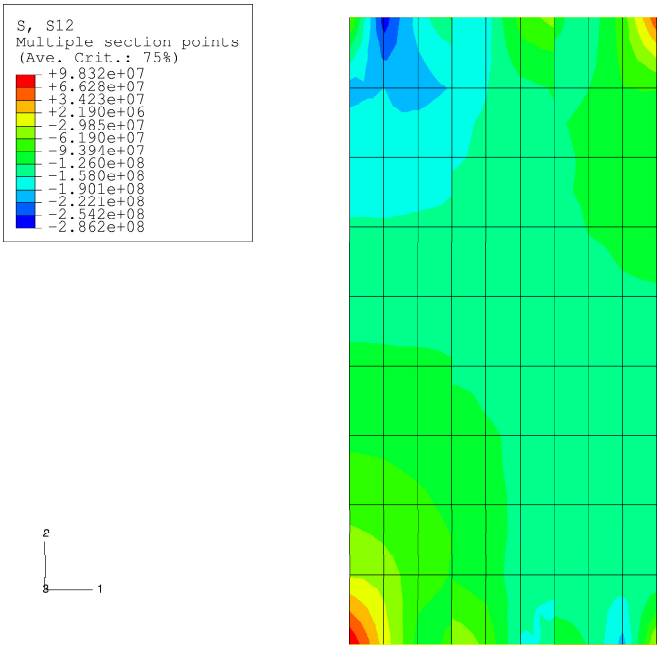

Figure 5.22: Unsmoothed shear stress (τ_{xy}) distribution in the web after the final iteration

has a value of $\alpha_{prin} = 40.2$ degrees, compared to the measured value of the chemically milled sheet $\alpha^{ct} = 45.4$ degrees.

In Table 5.4 additional output data from the Grisham algorithm is listed for the mid bay but with no measured data available for comparison. Panels 1 and 3 are ignored due to edge effects from the finite element analysis.

	Panel 2
k	0.552
α [degrees]	37.4
τ_{xy} [MPa]	-132.8
$\sigma_{x_{DT}}$ [MPa]	95.81
$\sigma_{y_{DT}}$ [MPa]	56.08
σ_{x_c} [MPa]	-3.16
σ_{y_c} [MPa]	-6.86

Table 5.4: Output data from the Grisham algorithm

The initial sheet buckling stress was impossible to determine from the tests as the extremely thin sheet would become unstable while the test piece was mounted in the machine.

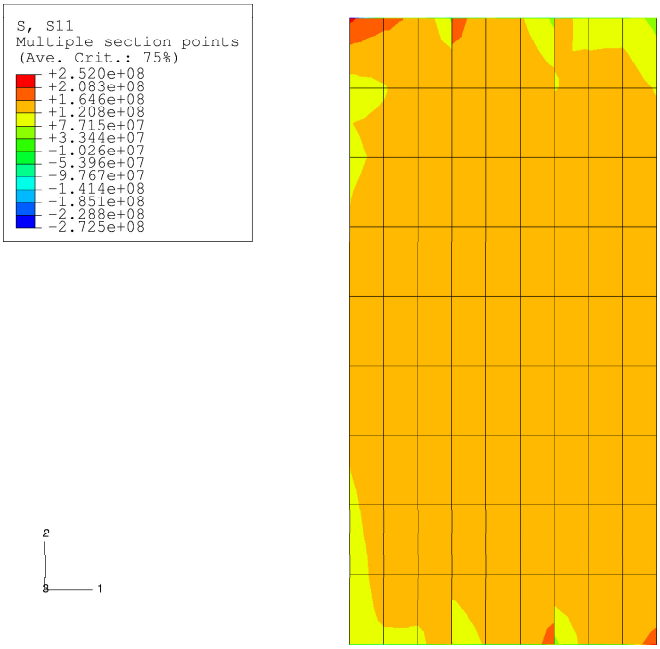

Figure 5.23: Unsmoothed normal stress (σ_x) in the web after the final iteration

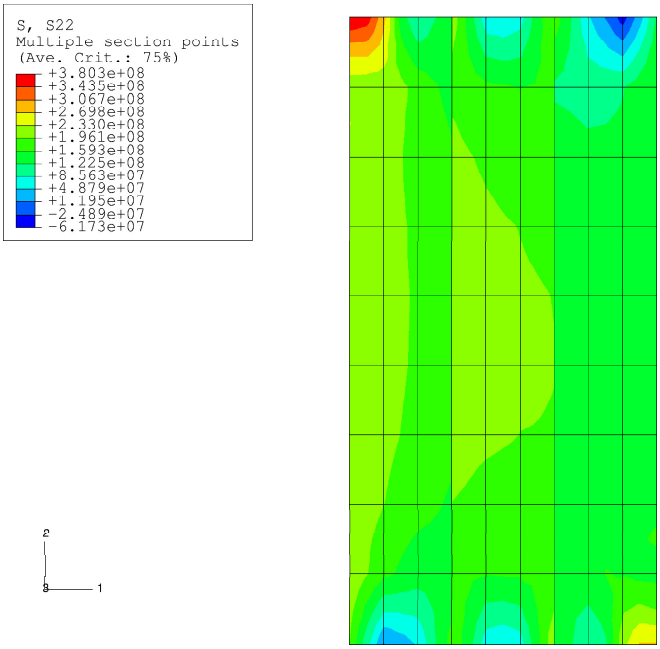

Figure 5.24: Unsmoothed normal stress (σ_y) in the web after the final iteration

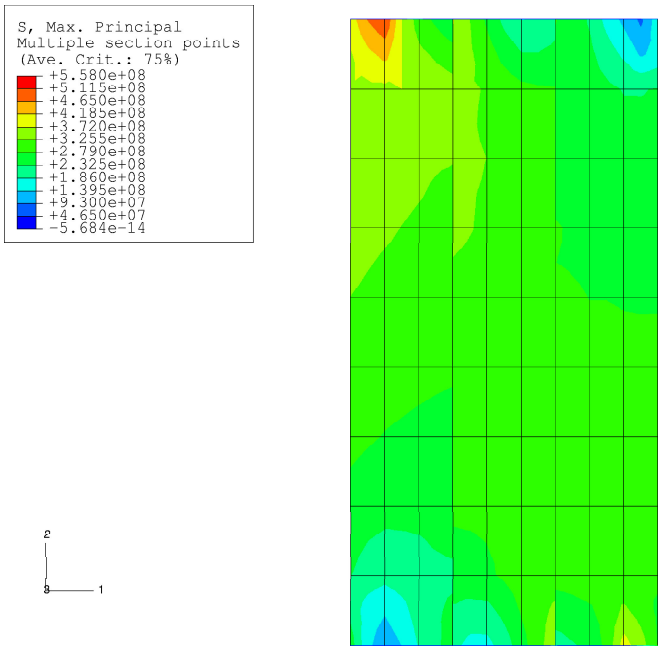

Figure 5.25: Unsmoothed maximum principal stress (σ_1) in the web after the final iteration

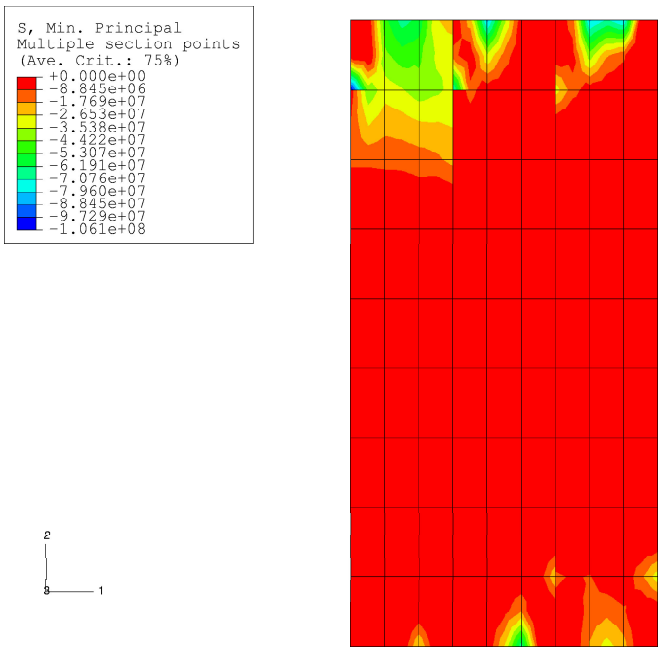

Figure 5.26: Unsmoothed minimum principal stress (σ_2) in the web after the final iteration

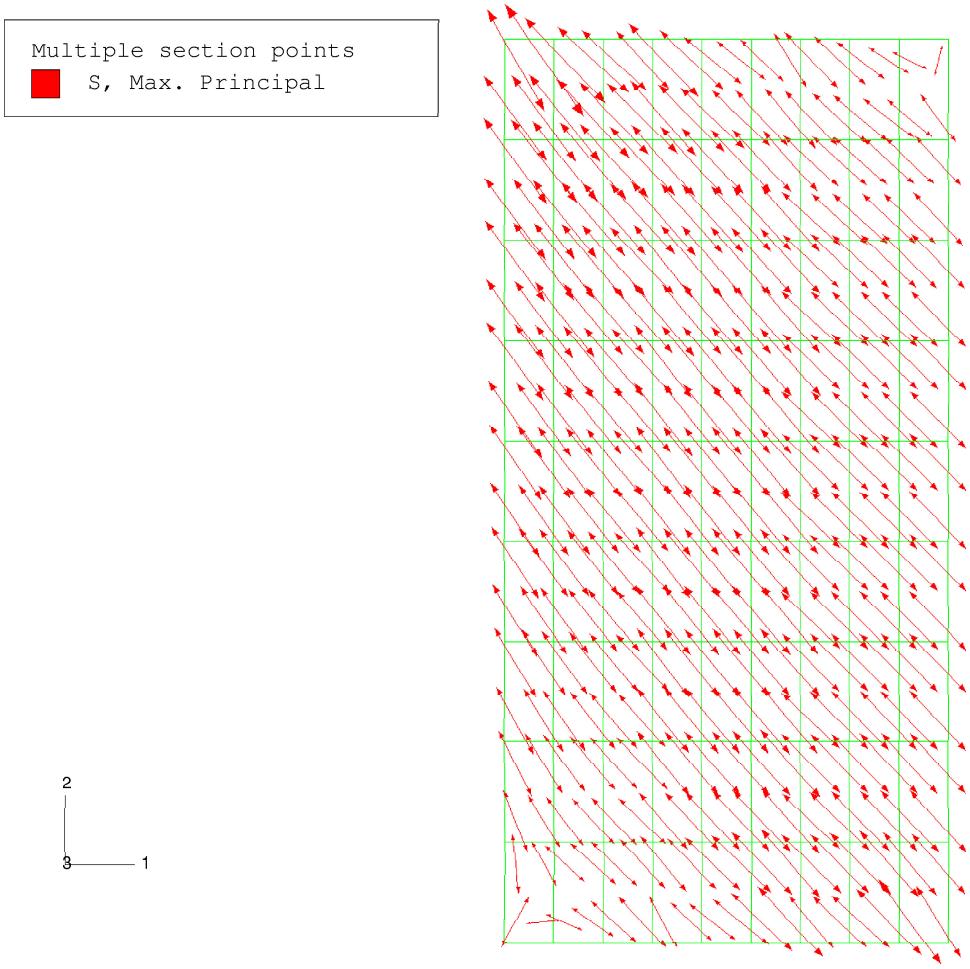

Figure 5.27: Maximum principal stress vectors in the web after the final iteration

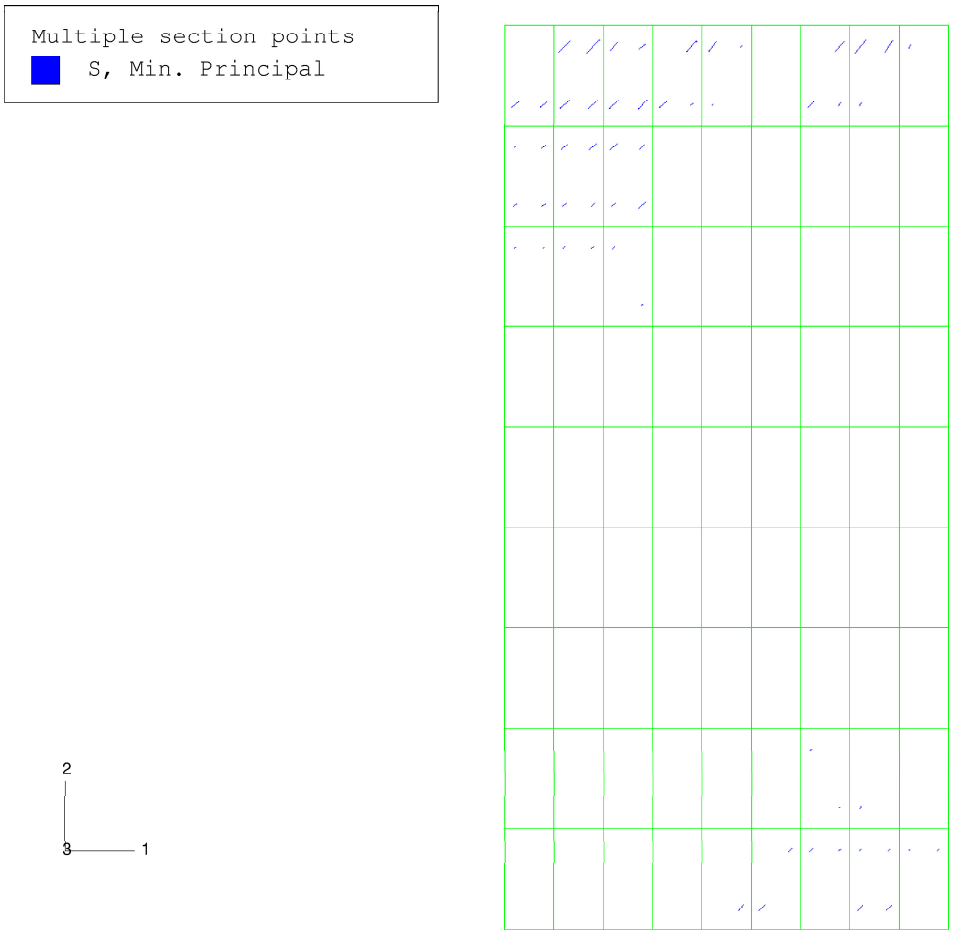

Figure 5.28: Minimum principal stress vectors in the web after the final iteration

5.2.3 Upright results

Axial strains in one stiffener adjacent to the middle panel were measured at three cross-sections along the length of the stiffener (See Figure 5.21). These values remained constant as the applied load increased up to about half the failure load.

Figure 5.29 shows the measured results for the longitudinal stresses at the mid-length of the stiffener. These measurements were taken on one of the uprights adjacent to the center panel. The yellow line represents the reading from strain gauge '41' which is placed on the land of the sheet. The blue line represents the reading from strain gauge '42' which is placed on the free surface of the attached stiffener leg. The orange line represents the reading from strain gauge '43' which is placed on the outside surface of the outer stiffener leg. Since the readings of these three gauges show good agreement, there are no significant bending effects, even though the upright is eccentric. Average upright stresses will therefore be compared. From the graph in Figure 5.29 the stress values at a load of 22 151 N ($\frac{P^m}{P^m_{ult}} = 0.5$ in the figure) for the three strain gauges are:

1. '41': σ_u = -9.5 ksi (-68.95 MPa)
2. '42': σ_u = -7 ksi (-48.26 MPa)
3. '43': σ_u = -7.5 ksi (-51.71 MPa)

The average value of these measured stresses is $\overline{\sigma}_u$ = -56.34 MPa. The average stress in upright number 2 of the Grisham approach is $\overline{\sigma}_u$ = -73.90 MPa. The average was calculated from all the section points at the integration points along the upright length.

5.2.4 Deflection results

Figure 5.30 shows the displaced shape of the finite element model after the final iteration. Figure 5.31 shows plots of the equivalent shear stiffness G^p_{IDT} and G^{ct}_{IDT}. G^p_{IDT} is computed using equations 31.a and 31.b in NACA TN 2661[3] and is represented by the blue dotted line. $G^{ct}_{IDT'}$ is the equivalent shear stiffness calculated from the test data. $G^{ct}_{IDT'} = \frac{P^m}{h_c \times t \times \gamma_{IDT}}$, where $\gamma_{IDT} = \frac{Gauge3 - Gauge4}{d}$. Gauges 3 and 4 are dial gauges used for measuring deflections at two locations on the test specimen. See Figure 5.21 for the locations of the dial gauges. G^{ct}_{IDT} is represented by the orange line on the graph. At $\frac{P^m}{P^m_{ult}}$ a value of $\frac{G^{ct}_{IDT}}{G} = 0.56$ is obtained. With a shear modulus of 25.98 GPa for 7075-T6 aluminium alloy, the equivalent modulus calculated from the measured data is G^{ct}_{IDT} = 14.55 GPa. Substituting the values for d and h_c into the above equations and solving for the difference between the two gauge readings, a value of Gauge 3 - Gauge 4 = 2.93 mm is obtained. In order to compare this measured difference to the finite element analysis results, displacement values at the nodes, corresponding to the locations on test specimen C were extracted and found to be: $u_{2_{gauge3}}$ = 2.81 mm and $u_{2_{gauge4}}$ = 5.14 mm which gives a difference of 2.33 mm. This is 20 % lower than the measured value of 2.93 mm.

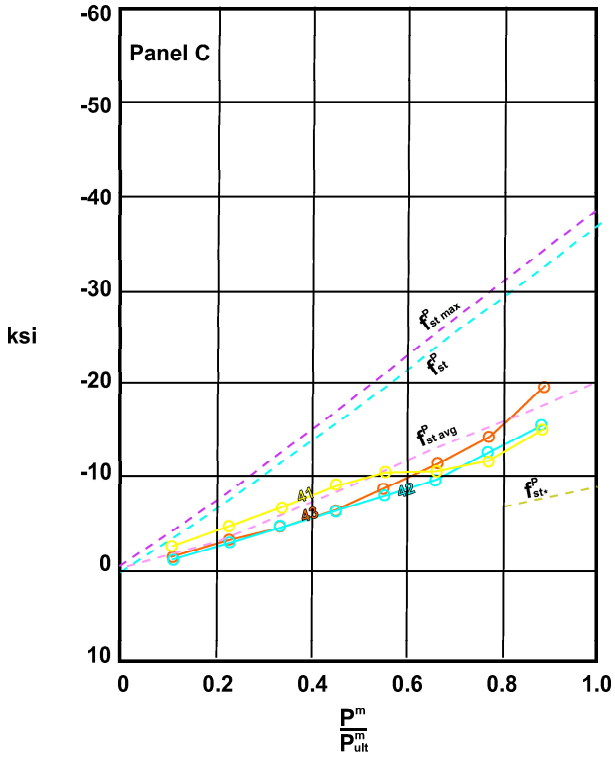

Figure 5.29: Measured longitudinal stresses at the mid-length of the stiffener (Reproduced from [13])

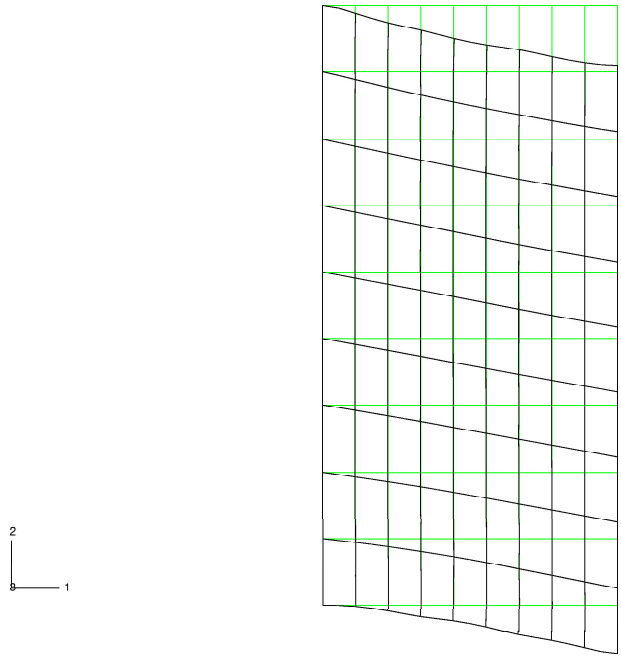

Figure 5.30: Displaced shape of the finite element model after the final iteration

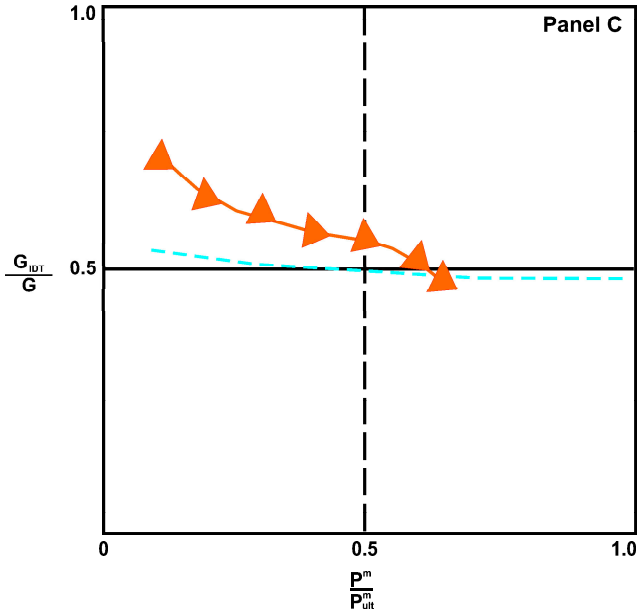

Figure 5.31: Shear stiffness variation as a function of load (Reproduced from [13])

5.3 Example 3 [14]

This example, like the two before, is a cantilever beam. Figure 5.32 gives the dimensional and geometric detail. The approach followed in [14] is to model diagonal tension by using a single model for multiple load conditions. As with the Grisham algorithm, the stiffness matrix is formulated once only. The method uses the induced strain concept in conjunction with an iterative procedure to enforce a condition of limited compressive principal stress within the thin membrane elements. Only a pure diagonal tension (PDT) condition is considered in this approach.

5.3.1 The finite element model

The webs are modelled using second order membrane elements while the bars are modelled using second order truss elements. A vertical load of 10 kips (44.48 kN) is applied at the free end of the beam. The mesh of the finite element model is shown in Figure 5.33. The critical buckling shear stress for this example is $\tau_{cr} = 18.66$ MPa which is much higher than that of any of the previous three examples. Figures 5.34, 5.35 and 5.36 show the stress results in the web at the end of the analysis. Figure 5.37 shows a vector plot of the maximum principal stress in the web while Figure 5.38 shows a vector plot of the minimum principal stress.

5.3.2 Web results

The only variable used in this comparative study is the diagonal tension angle. The results are shown in Table 5.5. Table 5.6 gives additional output data from the Grisham algorithm,

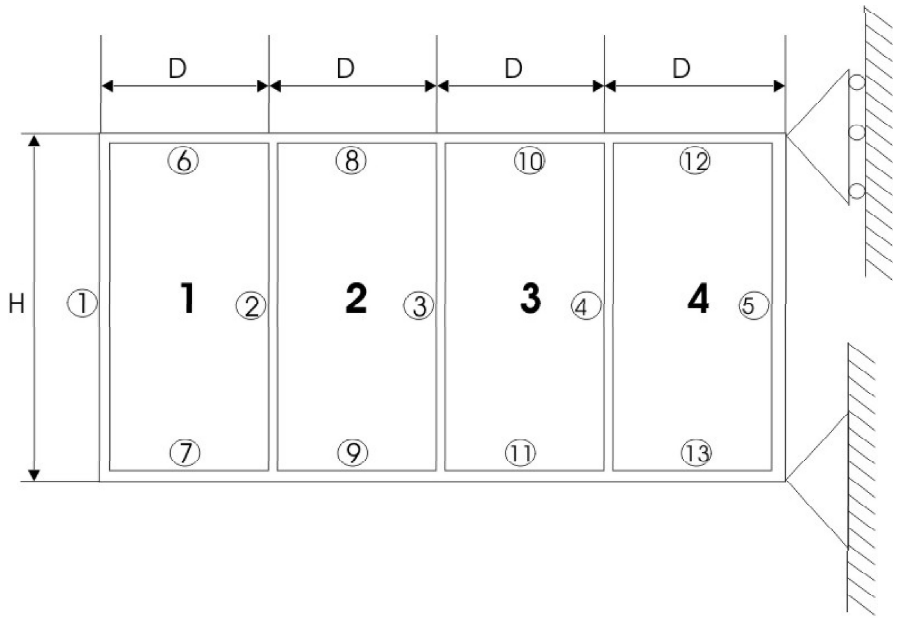

Bar areas (in)

$A_{1,6,7} = 0.3$
$A_{2\text{-}5} = 0.2$
$A_{8,9} = 0.4$
$A_{10,11} = 0.5$
$A_{12,13} = 0.6$

$T = 0.04$ in
$D = 6$ in
$H = 10$ in
$E = 10.5 \times 10^6$ PSI
$\nu = 0.3$

○ Bar

Figure 5.32: Cantilevered shear beam (Reproduced from [14])

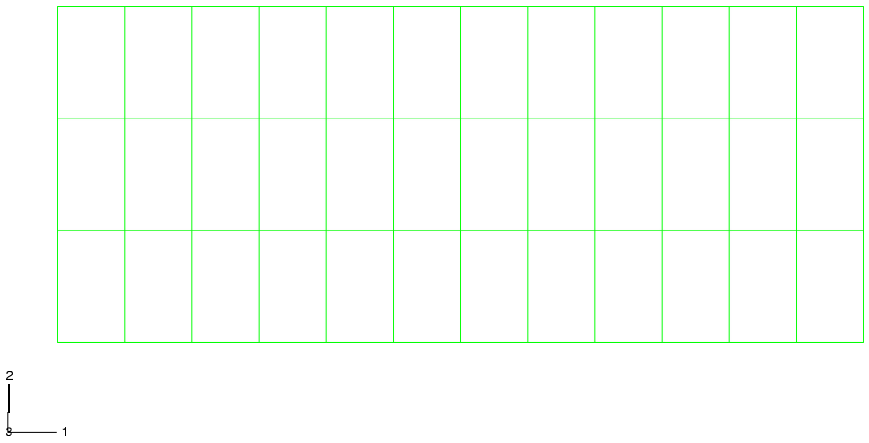

Figure 5.33: Mesh of finite element model

but with no measured data available for comparison.

	Panel 1	Panel 2	Panel 3	Panel 4
Grisham algorithm	44.37	44.00	43.77	43.70
Induced strain approach [14]	47.9	44.6	44.5	40.7
NACA approach [3]	46.9	44.3	43.6	43.0

Table 5.5: Diagonal tension angle α (degrees) comparison

5.3.3 Deflection data

The displaced shape of the beam at the end of the iterative analysis is shown in Figure 5.39.

5.4 Discussion

From the results of the example problems in this chapter as well as the results from the verification example in Chapter 2, it is evident that the Grisham algorithm yields good correlation with the worked examples and experimental data from the literature. As a tool during initial design iterations, it is certainly promising.

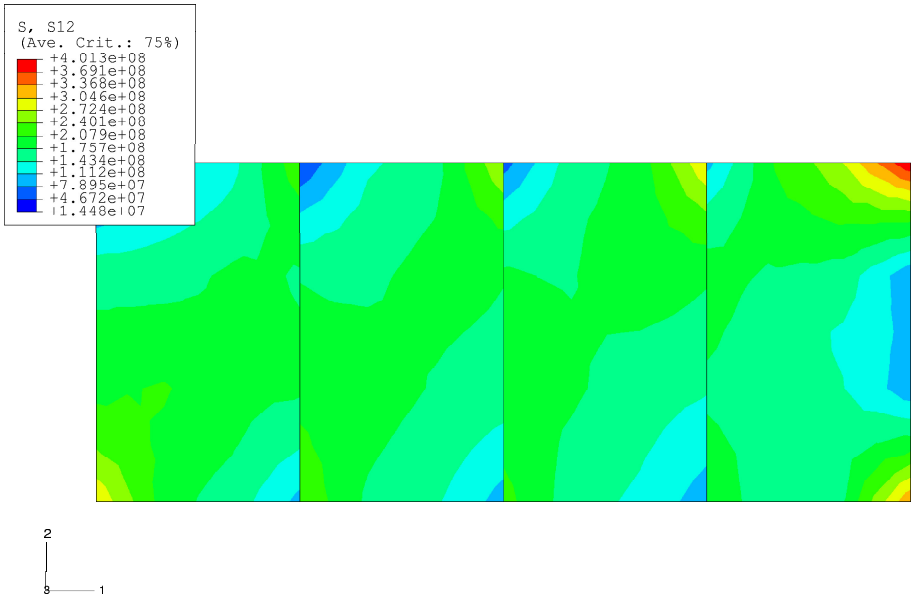

Figure 5.34: Unsmoothed shear stress (τ_{xy}) distribution in beam after the final iteration

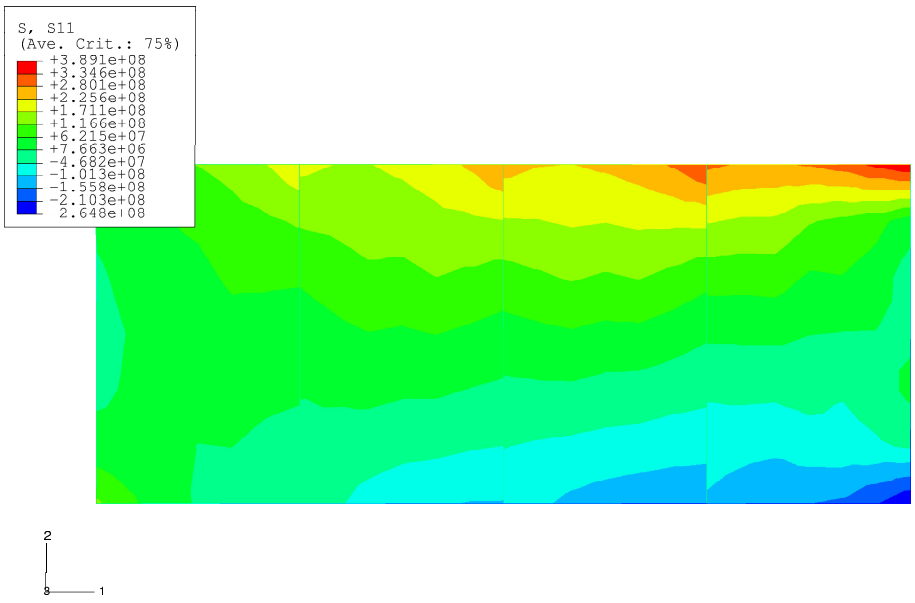

Figure 5.35: Unsmoothed normal stress (σ_x) in the beam after the final iteration

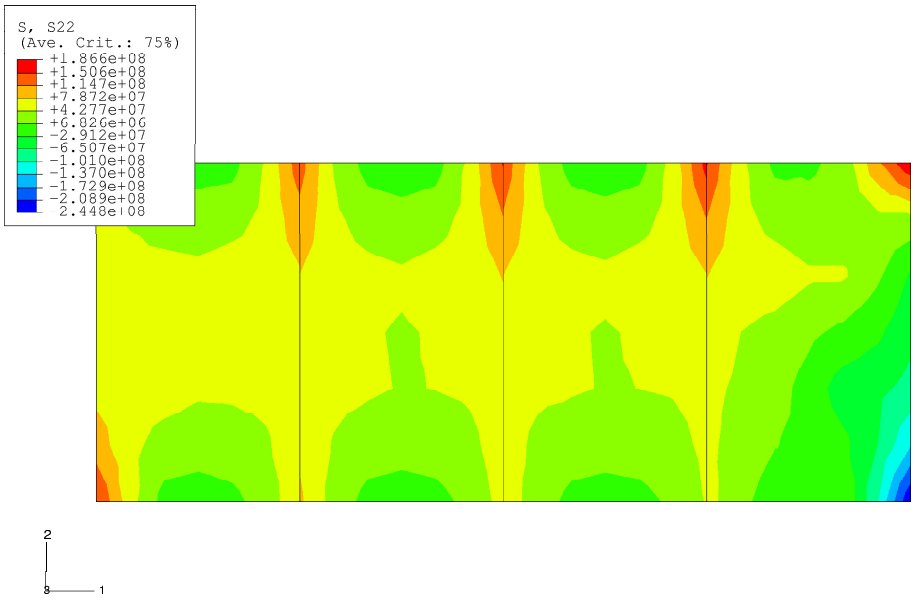

Figure 5.36: Unsmoothed normal stress (σ_y) in the beam after the final iteration

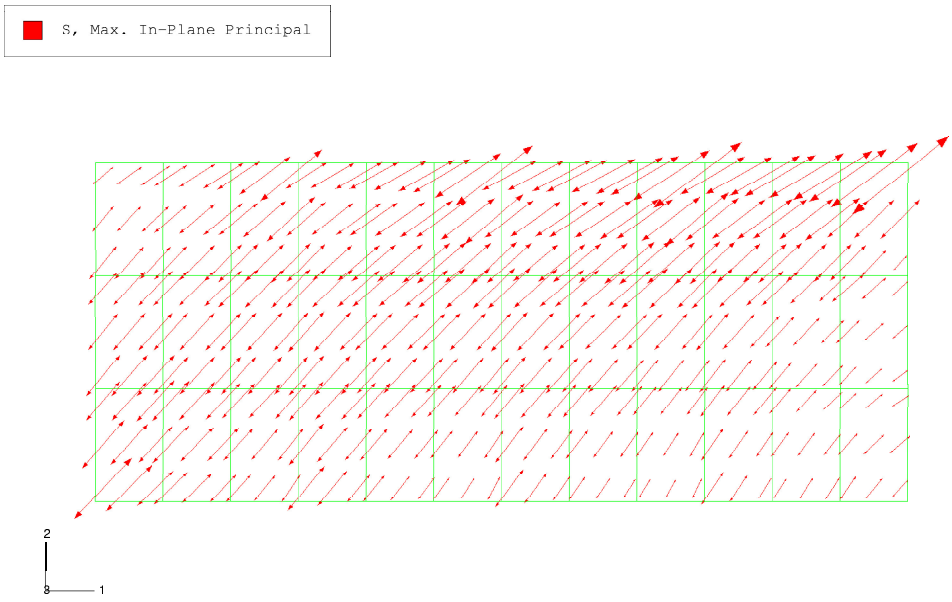

Figure 5.37: Maximum principal stress vectors in the web after the final iteration

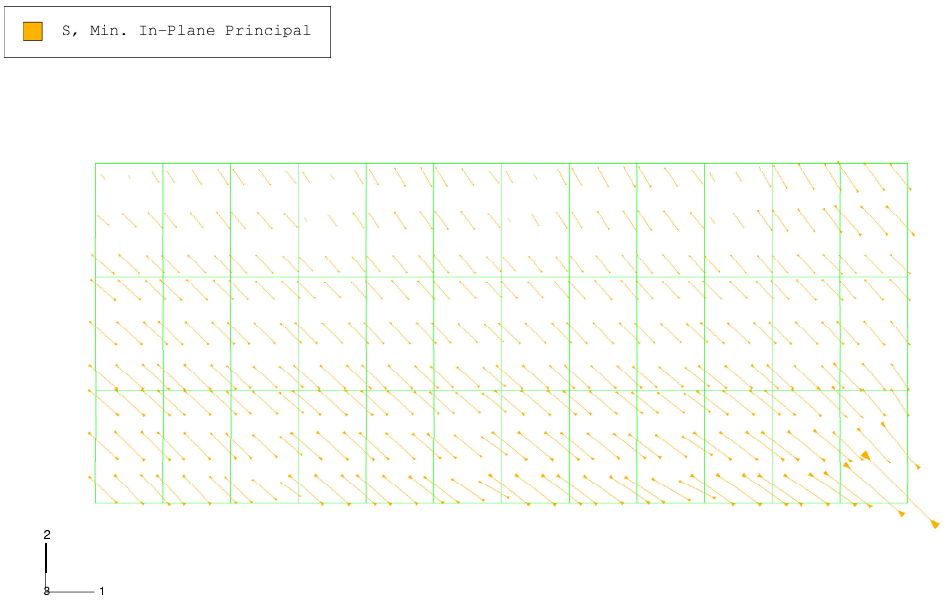

Figure 5.38: Minimum principal stress vectors in the web after the final iteration

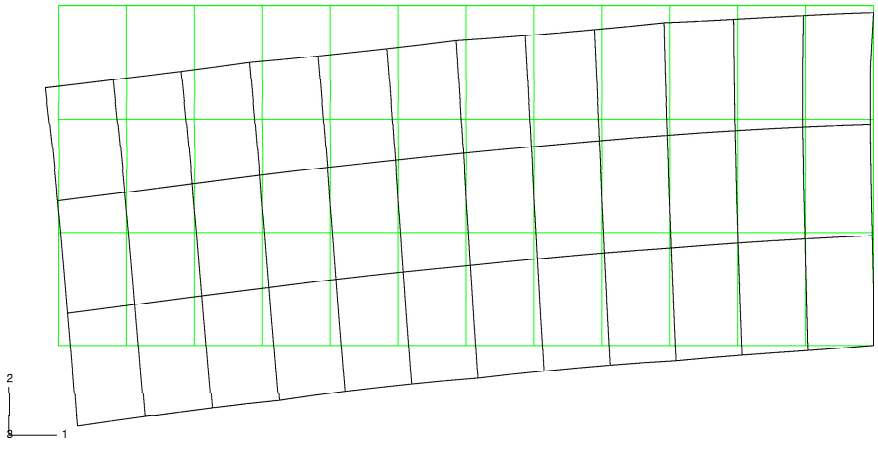

Figure 5.39: Displaced shape of the finite element model after the final iteration

	Grisham algorithm			
	Panel 1	Panel 2	Panel 3	Panel 4
k	0.403	0.413	0.409	0.372
τ_{xy} [MPa]	172.45	172.39	172.38	172.55
$\sigma_{x_{DT}}$ [MPa]	71.00	73.81	73.72	67.23
$\sigma_{y_{DT}}$ [MPa]	67.98	68.84	67.66	61.43
σ_{x_c} [MPa]	4.04	2.14	2.76	6.57
σ_{y_c} [MPa]	3.01	3.15	3.15	7.61

Table 5.6: Grisham algorithm web results